Apoptosis in the Rat Lens after In Vivo Threshold Dose Ultraviolet Irradiation

Ralph Michael,[1,2] *Gijs F. J. M. Vrensen,*[2,3] *Jan van Marle,*[4] *Lisha Gan,*[1] *and Per G. Söderberg*[1]

Purpose. To investigate DNA damage in the rat lens after in vivo close-to-threshold exposure to ultraviolet radiation (UVR).

Methods. Sprague-Dawley rats received 5 kJ/m^2 UVR (λ_{MAX} = 300 nm, $\lambda_{0.5}$ = 10 nm) unilaterally for 15 minutes. Animals were killed at 1, 6, and 24 hours and at 1 week after exposure. DNA-strand breaks were investigated in sagittal paraffin sections using the TdT-dUTP terminal nick-end labeling (TUNEL) technique and propidium iodide for counterstaining. Other lenses were prepared for transmission electron microscopy (TEM).

Results. TUNEL-positive nuclei were found at only 24 hours after UVR exposure. About one tenth of the epithelial cell nuclei were TUNEL positive, and affected cells were scattered over the entire epithelium. No TUNEL-positive cells were found at 1 or 6 hours or at 1 week after UVR exposure or in the nonexposed lenses. TEM verified the occurrence of programmed cell death and showed the breakdown of the apoptotic cells by adjacent cells. No signs of necrosis were found.

Conclusions. Threshold-dose UVR induces programmed cell death that peaks 24 hours after exposure and involves the entire epithelium. Dead cells are removed from the epithelium by phagocytosis. (*Invest Ophthalmol Vis Sci.* 1998;39:2681-2687)

In the current study, the effects of in vivo ultraviolet radiation (UVR)-induced DNA damage on the lens epithelium in rats was investigated and are reported here. The chronology, localization, and morphology of programmed cell death were studied.

Epidemiologic studies[1,2] and experimental studies in rats, mice, rabbits, and squirrels[3-9] show a relationship between UVR exposure and subsequent lens opacities. Morphologically, these events correspond to swelling and disruption of lens epithelial cells and cortical lens fibers.[5,9] Swollen mitochondria, subcapsular vacuoles, and chromatin condensation and nuclear fragmentation are found in the epithelium.[5] Epithelial hyperplasia is observed after long-term or above-threshold exposure.[5,10]

The UVR dose applied in the current experiments (5 kJ/m^2 at 300 nm) is close to threshold for cataract in rabbits and rats.[3,11] Previous experiments have shown that the mean forward light scattering in the lens increases during the first week and remains constant up to 32 weeks after exposure.[6,11]

The wavelength in the current experiment was chosen according to biological and environmental significance. Within the lens, the epithelium receives the highest dose of UV-B radiation (280-315 nm) incident to the eye.[12] The UV-B radiation is strongly absorbed by lens proteins and DNA and therefore potentially has a damaging effect on the lens epithelium.[13] Epithelial damage is critical for lens growth and transparency because the lens epithelium is involved in the maintenance of water, ions, and metabolite homeostasis, and its germinative cells are the source of lens fiber cells. Terrestrial solar UVR varies most around the wavelength of 300 nm, depending on the latitude, the time of day, and the stratospheric ozone concentration. The annual maximum value at 300 nm at the Canary Islands (28°N) is about seven times higher than the maximum reached in Stockholm (59°N).[14,15]

Ultraviolet radiation and other chemical or physical agents can cause different stresses to a tissue and can finally induce cell death. Low-dose stress to a tissue may not directly kill cells but can cause damage to DNA, cell membranes, or other cell organelles. Such damage either may be repaired if the cell survives or may lead to programmed cell elimination, apoptosis, or programmed cell death. With high-dose stress, the agent may kill the cell directly with no possibility for cell survival.[16]

In this article the term "apoptosis" is used as a morphologic descriptor of programmed cell death. The main characteristics of apoptotic morphology are condensation and fragmentation of the cellular content as seen in electron microscopy.[17] Another key event with programmed cell death is the double-strand cleavage of DNA into fragments that are multiples of 180 bp to 200 bp.[18] This cleavage of the DNA can be visualized by agarose gel electrophoresis or via in situ marking of free 3′-OH-DNA ends with the TdT-dUTP terminal

From the [1]Karolinska Institutet, St. Erik's Eye Hospital, Stockholm, Sweden; [2]The Netherlands Ophthalmic Research Institute, Amsterdam, The Netherlands; the [3]Department of Ophthalmology, State University of Leiden, The Netherlands; and the [4]Department of Electron Microscopy, Academic Medical Center, University of Amsterdam, The Netherlands.

Supported by Gottlieb Daimler-und Karl Benz-Stiftung, Ladenburg, Germany; and St. Erik's Ögonforskningsstiftelse, Anders Otto Swärds Stiftelse, Carmen och Bertil Regnérs Stiftelse, Erik och Edith Fernströms Stiftelse, Karolinska Institutets Forskningsstiftelser, Loo och Hans Ostermans Stiftelse, and Svenska Sällskapet för Medicinsk Forskning, Stockholm, Sweden.

Submitted for publication February 23, 1998; revised June 15, 1998; accepted July 31, 1998.

Proprietary interest category: N.

Reprint requests: Ralph Michael, Research Laboratory, St. Erik's Eye Hospital, S-112 82 Stockholm, Sweden.

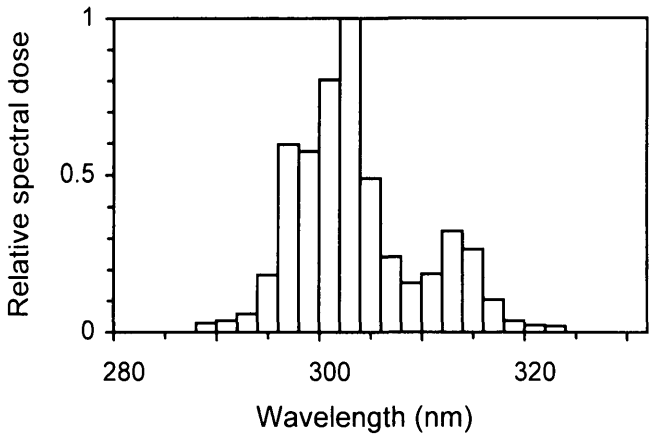

FIGURE 1. Relative spectral dose in the corneal plane of the exposed eye. The total dose between 285 nm and 325 nm was 5 kJ/m^2.

nick-end labeling (TUNEL) assay. However, this assay is capable of detecting nonapoptotic DNA-strand breaks also, such as those induced, for instance, by repair enzymes after oxidative stress.[16,19] Therefore, the TUNEL assay always should be accompanied by morphologic investigations to verify programmed cell death.[20]

Apoptotic morphology and DNA fragmentation after UVR exposure have been demonstrated previously in the lens epithelium.[21] However, the role of programmed cell death in human cataractogenesis is still controversial. Harocopos and coworkers[22] detected no evidence of apoptotic cells in the epithelium of capsulorhexis specimens and only limited evidence in epithelial whole mounts of human cataractous lenses. However, Li et al.[23] found a large number of apoptotic cells in capsular epithelial cell samples of human cataractous lenses obtained from the operation theater and only a few in normal lenses obtained from donors.

METHODS

The 6-week-old Sprague-Dawley rat was the animal model used. One eye of each rat was exposed in vivo to UVR. At different time points after UVR exposure, DNA-strand breaks in the lens were labeled, and lens morphology was studied by light and transmission electron microscopy (EM).

UVR Exposure

The radiation from a high-pressure mercury lamp (HBO 200 W; Osram) was collimated, passed through a water filter and then an interference filter (λ_{MAX} = 300 nm; half bandwidth, 10 nm), and, finally, projected on the cornea of one eye.[24] The spectrum of the radiation is given in Figure 1. Altogether, 18 female Sprague-Dawley rats were exposed to radiation unilaterally at the age of 6 weeks. Ten minutes before the exposure, the animal was anesthetized by intraperitoneal injection of a mixture of 94 mg/kg ketamine and 14 mg/kg xylazine. Five minutes after injection, the mydriaticum tropicamide was instilled in both eyes. After another 5 minutes, the eye was exposed to 5 kJ/m^2 UVR for 15 minutes with a narrow beam that covered only the cornea and the eye lids of the exposed eye.

Altogether, 12 animals used for DNA analysis and light microscopy were divided into four groups and kept 1, 6, or 24 hours or 1 week after UVR exposure. Transmission EM was performed at 24 hours and 1 week after exposure, with three animals each. The rats were killed by carbon dioxide exposure followed by cervical dislocation. All animals were kept and treated in accordance with the ARVO Statement for the Use of Animals in Ophthalmic and Vision Research.

TUNEL Assay and DNA Staining

Five minutes after lens extraction and at a maximum of 15 minutes after death, the isolated lenses were fixed in 4% paraformaldehyde in phosphate-buffered saline for 4 hours at 6°C. Lenses were dehydrated with ethanol and routinely embedded in paraffin. Axial sections (4 μm) were dewaxed with xylene and rehydrated. The lens sections were microwaved in 200 ml citrate buffer for 1 minute at 750 W and rapidly cooled to achieve permeabilization,[25] which reveals epitopes on the DNA to make it accessible for the TUNEL assay.

Labeling of DNA-strand breaks was performed using the In Situ Cell Death Detection Kit-Fluorescein (No. 1 684 795; Boehringer-Mannheim) according to the manufacturer's protocol. Terminal deoxynucleotidyl transferase (TdT) was used to catalyze the polymerization of fluorescein-conjugated dUTP to free 3′-OH-DNA ends (TUNEL method). All tissue slides were treated in one batch for permeabilization and TUNEL assay. Positive and negative controls were always included in the batch. In positive controls, DNA-strand breaks were induced by applying 1 mg/ml DNase I in reaction buffer (No. 104 159; Boehringer-Mannheim) for 10 minutes at room temperature before the TUNEL assay. For negative controls, the fluorescein-dUTP was applied without the enzyme TdT in the reaction medium. All lens sections treated for the TUNEL assay were subsequently stained with 5 μg/ml propidium iodide (P 4170; Sigma) in phosphate-buffered saline for 15 minutes at 37°C.[26]

Confocal Microscopy

The fluorescent slides were mounted with antifade Vectashield (Vector Laboratories, Burlingame, CA) and viewed using a confocal microscope (Leica Laser Technik GmbH).

The emissions from fluorescein (excitation at 488 nm; detection with band pass filter 530 ± 10 nm) and propidium iodide (excitation at 563 nm; detection with high pass filter at 610 nm) were scanned simultaneously by two photomultipliers. The sensitivity range was set by appropriate selection of photomultiplier voltage and offset. The acquired images were stored as TIFF (tagged image file format) files with 512 × 512 pixel format. All microscope parameters were kept constant in a series of images to allow direct comparison of the fluorescence intensities.

FIGURE 3. Confocal image of mid-sagittal sections of the lens epithelium with fluorescein-TdT-dUTP terminal nick-end labeling (TUNEL) signal (**A**, **D**) and propidium iodide signal (**B**, **E**). The same field is displayed as a combined image of fluorescein-TUNEL and propidium iodide (**C**, **F**). The *inset* in (**C**) gives the color coding for each pixel in the combined images depending on the fluorescein-TUNEL intensity (*ordinate*) and the propidium iodide intensity (*abscissa*). Scale bars, 10 μm.

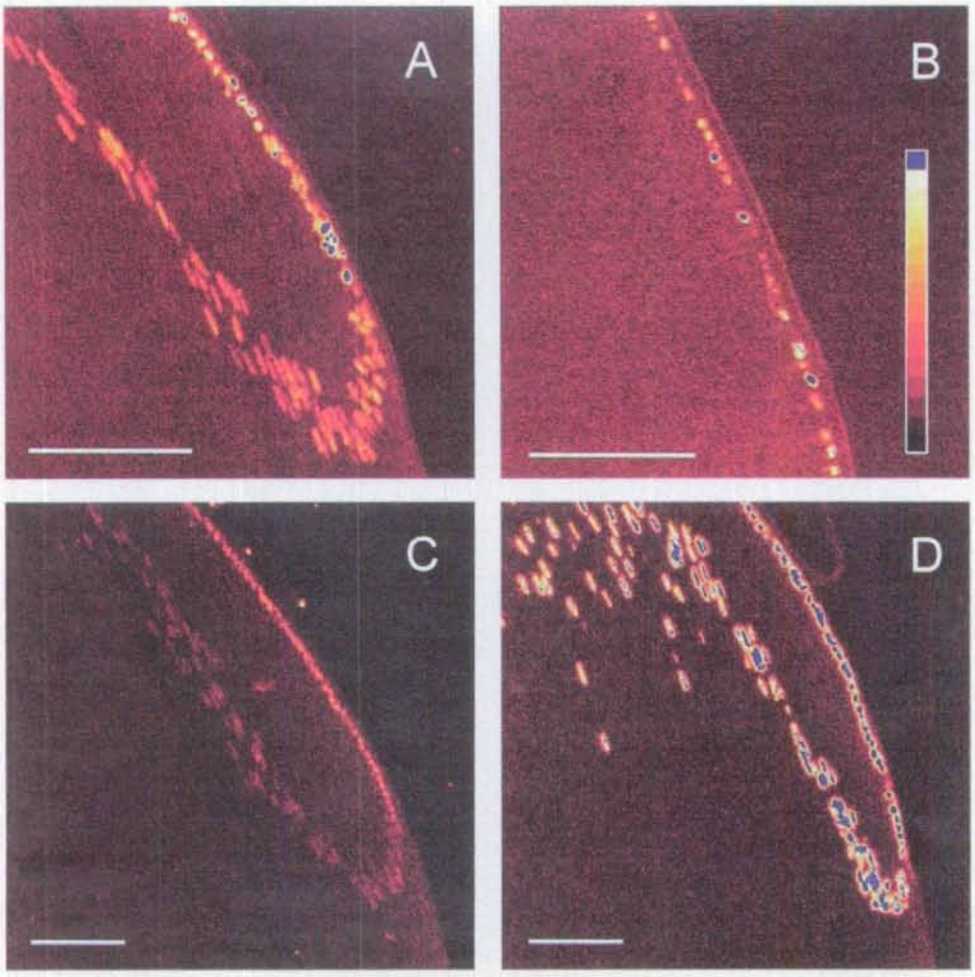

FIGURE 2. Pseudocolor confocal images of mid-sagittal lens sections with fluorescein–TdT-dUTP terminal nick-end labeling (TUNEL) staining. Highest fluorescent intensities are shown in blue and are considered TUNEL positive. **(A)** Equatorial region of the lens, 24 hours after ultraviolet radiation exposure; **(B)** the anterior pole region of the same lens section; **(C)** a nonexposed contralateral lens; and **(D)** a lens section treated with DNase I before the TUNEL assay, which serves as a positive control. Scale bars, 100 μm.

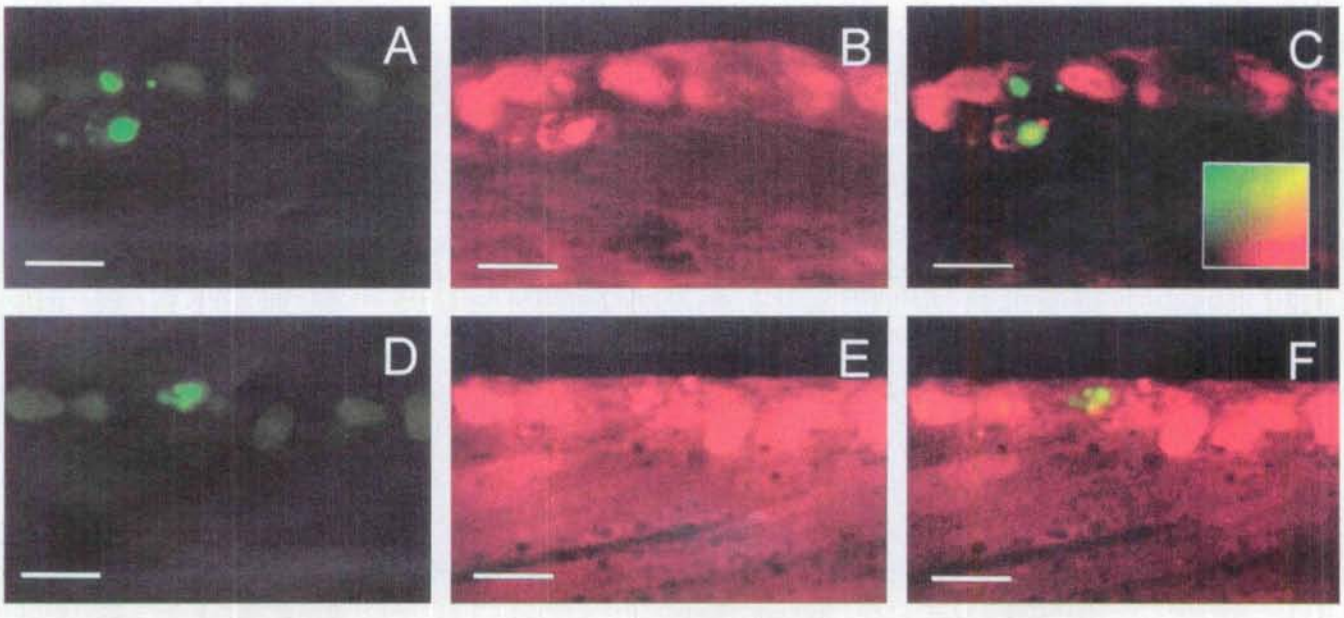

The images are displayed in pseudocolor, ranging from white (high intensity) via yellow and orange to brown and black (low intensity). Intensities above the selected dynamic range (>255) are shown in blue (Fig. 2).

The confocal images can also be displayed in other lookup tables, that is, single color green or red, that mimic fluorescein or propidium iodide fluorescence, respectively (Figs. 3A, 3B and 3D, 3E). Images of fluorescein and propidium iodide from the same tissue area can be combined and displayed with a new lookup table (Figs. 3C, 3F). For calculation of combined fluorescein and propidium iodide fluorescence, the Multicolor Analyzing Software (Leica Laser Technik) was used. A location with a high intensity of fluorescein and propidium iodide is shown in yellow, a location with a high intensity of only fluorescein is shown in green, and a location with a high intensity of only propidium iodide is shown in red (Fig. 3C).

Light Microscopy and Transmission EM

Paraffin lens sections adjacent to those used for the TUNEL assay were dewaxed and stained with hematoxylin and eosin and viewed in a light microscope. Other isolated lenses were fixed in Peters fixative (0.08 M cacodylate-buffered solution of 1.25% glutaraldehyde and 1% paraformaldehyde, pH 7.3)[27] for at least 7 days at 6°C. Dissected lens regions were postfixed in 1% OsO_4 (Merck 24505) and 1.5% kaliumhexa-cyanoferrat (Merck 4973), dehydrated in ethanol, and embedded in epoxy resin. Sagittal sections of 80 nm to 100 nm were contrasted with uranyl acetate and lead citrate and studied in a Philips EM 201 electron microscope.

Results

All nuclei in the DNase I-treated lens sections were TUNEL positive (Fig. 2D). Figure 2D shows that all epithelial and lens fiber nuclei down to deep in the nuclear bow region contain DNase-sensitive DNA. All nuclei were also propidium iodide positive, showing that the DNA was in a double-strand configuration. After omission of TdT from the medium, no nuclei were TUNEL positive, indicating the absence of false-positive staining in the material.

TUNEL-positive cells were completely absent in the epithelium and lens bow in the lenses collected at 1 and 6 hours and at 1 week after irradiation and in all nonexposed contralateral lenses (Fig. 2C). At 24 hours after irradiation, TUNEL-positive cells were found to be scattered over the whole epithelium from the central anterior to the equatorial region, but no positive cells were found in the lens bow (Figs. 2A and 2B).

The percentage of TUNEL-positive cells at 24 hours after exposure was between 10% and 20% and appeared to be greater in the anterior than in the equatorial region of the epithelium. The average percentage of positive cells for three exposed lenses in two regions of the epithelium was as follows: equatorial/anterior = 12/16, 9/20, and 14/26. Clusters of TUNEL-positive cells were frequently seen in the germinative zone (Fig. 2A).

Condensation and fragmentation of deranged TUNEL-positive material were frequently observed in epithelial nuclei at 24 hours after irradiation (Fig. 3). Sometimes these nuclei were found between the epithelial monolayer and the fibers (Figs. 3A, 3B, 3C).

Electron microscopy (Figs. 4 and 5) and light microscopy verified the chronology and localization of apoptosis. Apoptosis was also observed in the postgerminative differentiation-elongation region (Fig. 6). No signs of necrosis, such as swelling of the nucleus or disruption of plasma membrane, were found. The electron micrographs showed apoptosis either as apoptotic cells with intact plasma membrane or as normal cells containing phagocytosed apoptotic bodies with distinct borders (Figs. 4, 5, 6). Apoptotic cells showed chromatin condensation (Fig. 4A) and were sometimes found to be engulfed by neighboring normal cells (Fig. 4B). Apoptotic bodies were frequently found inside normal cells (Figs. 4C, 4D). The series of different stages of apoptosis (Figs. 4A, 4B, 4C, 4D) indicates that adjacent cells were involved in the breakdown (phagocytosis) of the apoptotic cells.

Discussion

In vivo exposure to UVR induces programmed cell death in the rat lens epithelium. This is verified by positive in situ labeling of DNA-strand breaks with the TUNEL assay, by propidium iodide counterstaining, and by light microscopy and transmission EM, which clearly show apoptotic morphology.

The UVR-induced programmed cell death was observed to peak at 24 hours after exposure. This is consistent with observations in other tissues after exposure to UV-B radiation. For instance, in epidermal cells the time point for the maximum of DNA laddering was found to be between 12 and 24 hours after exposure.[28,29] In murine lymphoma cells, the DNA laddering starts at 8 hours after exposure; at 32 hours after exposure, 25% of the cells show apoptotic morphology.[30]

DNA damage and its subsequent repair as induced by UVR[31] or oxidative stress (H_2O_2)[32,33] occur immediately after the insult. However, at 1 and 6 hours after exposure we observed no DNA fragmentation with the TUNEL assay. The primary UVR-induced DNA damage may contain too few 3′-OH end strand breaks to be detected directly with the TUNEL assay, or the primary DNA damage can be repaired within 1 hour.[31-33] Cells with partial DNA damage may fail to function properly during transcription and mitosis[34] and may therefore be destined to undergo programmed cell death.

Previously, Godar[35] found that the chronology for apoptosis depends on the type of UVR. Long-wavelength UVR (340-400 nm) induced immediate apoptosis (0-4 hours after insult),[35,36] and short-wavelength UVR (200-320 nm) delayed apoptosis (>20 hours after insult).[35] It has been suggested that the type of initial damage (e.g., DNA or membrane) as induced by different wavelengths of UVR is determining different core mechanisms for programmed cell death.[30,35]

TUNEL-positive fragments were often found with intense propidium iodide counterstaining (light green to yellow color in Figs. 3C and 3F), which supports the concept that the TUNEL-positive cells we found do not just have a considerable number of DNA-strand breaks but that this DNA damage is a result of programmed cell death.

Typical apoptotic morphology was observed in transmission EM sections, showing chromatin condensation and membrane-bound apoptotic bodies (Figs. 4, 5). Figure 4 illustrates the different morphologic stages of programmed cell death[17]: formation of apoptotic bodies (Fig. 4A), phagocytosis (Fig. 4B), and, finally, degradation (Figs. 4C, 4D).

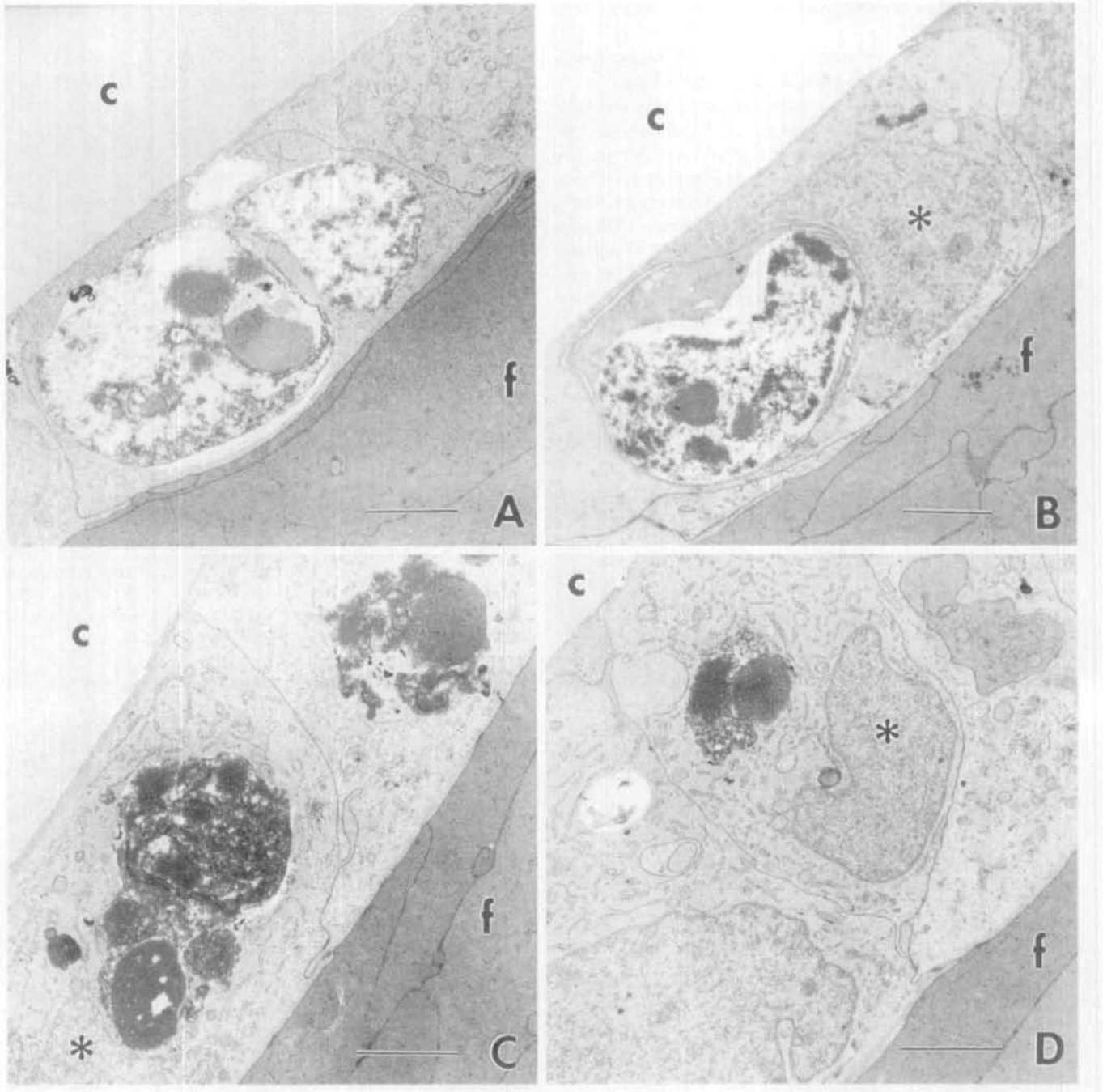

FIGURE 4. Transmission electron micrographs of epithelial cells 24 hours after exposure showing the phagocytosis of apoptotic cells. Apoptotic cell showing chromatin condensation (**A**), apoptotic cell with intact plasma membrane engulfed by its neighbor (**B**), several apoptotic bodies inside normal cells (**C**), and probable end stage of the phagocytosis (**D**). c, lens capsule; f, lens fiber; *, nucleus of the phagocytosing adjacent cell. Scale bars, 2 μm.

The formation of apoptotic bodies starts with chromatin condensation (Fig. 4A), which is often seen along the nuclear envelope (Figs. 4A, 4B). The formed apoptotic bodies are then phagocytosed by adjacent cells (Fig. 4B). The phagocytosis is characterized by the engulfment of the membrane bound apoptotic bodies by neighboring epithelial cells. Epithelial cells are known to be capable of phagocytosis.[17,18] In the lens epithelium, phagocytosis was seen previously only during embryonic development[37] or in vitro.[38,39] Inside the phagocytosing cell, the apoptotic bodies are further degenerated and digested (Fig. 4C). In the latest stage of phagocytosis, very condensed residual bodies are seen inside the phagocytosing cell (Fig. 4D).[17,40–43]

The time between the initial toxic event and the formation of apoptotic bodies is known to vary considerably.[16,18] Because the formation of apoptotic bodies and the phagocytosis are rather rapid,[16,18] it is possible that not all cells undergoing programmed cell death can be detected at 24 hours after exposure. Therefore, probably more than 10% to 20% of the epithelial cells might be involved in programmed cell death. Further experiments are needed to investigate the number of apoptotic cells in different regions of the epithelium and at

different times shortly before and after the time point 24 hours after exposure.

During the UVR exposure, the pupil of the rat's eye was dilated to achieve an equal pupil size. After instillation of mydriaticum tropicamide, the pupil diameter was approximately 90% of the coronary lens diameter. Therefore, the germinative zone was not directly exposed to UVR in the present experiment. Furthermore, recent experiments of our group[44] have shown that unpigmented rats receiving mydriatic drops (tropicamide) do not develop more cataracts than rats receiving miotic drops (pilocarpine) before UVR exposure. Therefore, the occurrence of TUNEL-positive cells in the germinative zone (Fig. 2A) suggests that the unpigmented iris does transmit parts of the UVR. Because of its high mitotic activity, this zone is probably more sensitive to UVR stress. Therefore, even UVR attenuated by the iris seems to be capable of inducing programmed cell death in the germinative zone. The clusterlike appearance of TUNEL-positive cells (Fig. 2A) is a common phenomenon with programmed cell death.[17] Its frequent occurrence in the germinative zone might also be explained by the high miotic activity. It could be speculated that cells undergoing mitosis are subject to programmed cell death and are therefore seen as clusters.

No nuclei in the nuclear bow showed apoptosis or TUNEL-positive staining. This indicates that UVB radiation does not reach down to the cells of the nuclear bow because of absorption of UVR in the overlying tissue.[13,45,46]

Apoptotic bodies are frequently seen as single fragments at the apical (fiber-facing) side of the epithelium between the epithelial monolayer and the lens fibers (Figs. 3A, 3B, 3C, and 5). This was observed previously in developmental cell death in the lens.[47] It is known that dying cells often lose cell-to-cell and cell-to-matrix contacts[48] and that they are extruded from the epithelium toward the apical side.[17,18,49,50]

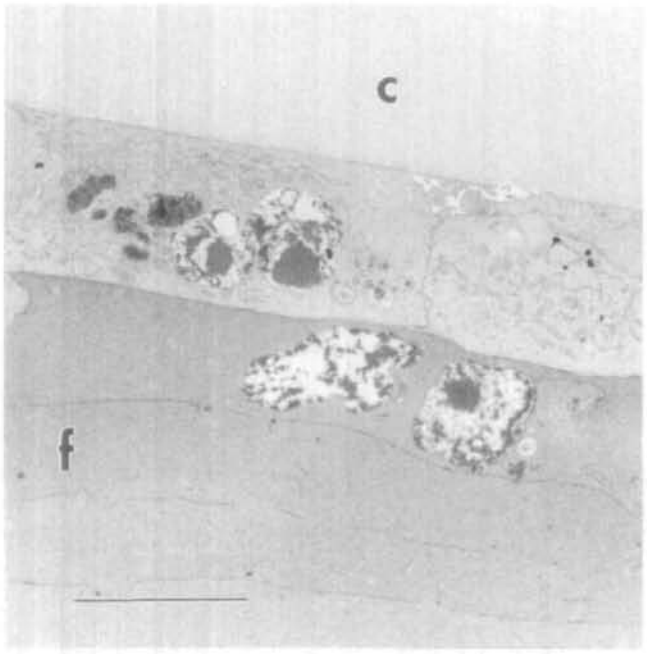

FIGURE 5. Transmission electron micrograph of epithelial cells 24 hours after exposure showing apoptotic bodies between the epithelial monolayer and the lens fibers. Scale bar, 5 μm. c, lens capsule; f, lens fiber.

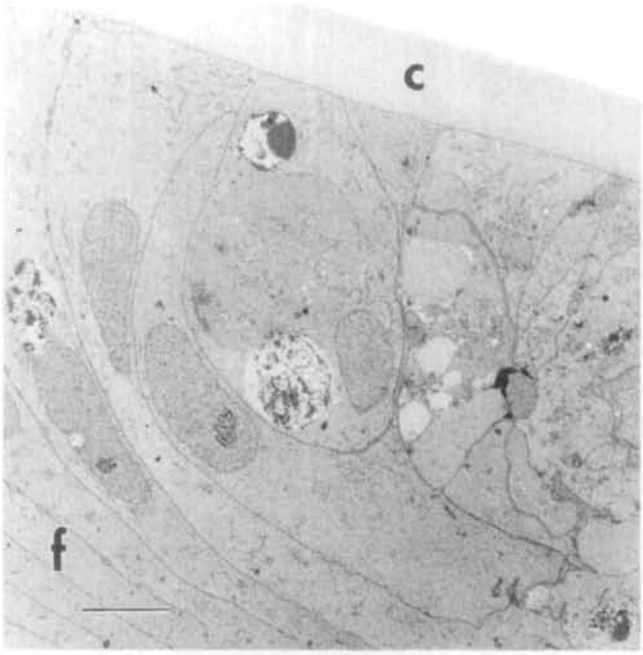

FIGURE 6. Transmission electron micrograph showing the postgerminative elongation zone of the epithelium 24 hours after exposure. Apoptotic bodies are seen inside normal cells; the right part of the figure shows an aggregation of epithelial cells. Scale bar, 5 μm. c, lens capsule; f, lens fiber.

CONCLUSIONS

Threshold-dose UVR induces programmed cell death that peaks at 24 hours after exposure and involves the entire lens epithelium. Dead cells are removed from the epithelium by phagocytosis. It seems most likely that after UVR exposure, lens epithelial cells undergo repair processes and that cells that fail to be repaired undergo programmed cell death. In this way, programmed cell death clears damaged cells. If such cells were to remain in the lens epithelium, they would most probably impair lens growth and transparency.

Acknowledgments

The authors thank Agneta Bonnevier (St. Erik's Eye Hospital, Stockholm, Sweden) for making the paraffin sections; Anneke de Wolf (The Netherlands Ophthalmic Research Institute, Amsterdam) for cutting ultrathin sections for TEM; and Marina Danzman and Niko Bakker (both of The Netherlands Ophthalmic Research Institute, Amsterdam) and Maud Leindahl (St. Erik's Eye Hospital, Stockholm, Sweden) for photographic assistance.

References

1. Taylor HR. Ultraviolet radiation and the eye: an epidemiologic study. *Trans Am Ophthalmol Soc.* 1990;87:802–853.
2. Cruickshanks KJ, Klein BE, Klein R. Ultraviolet light exposure and lens opacities: the Beaver Dam Eye Study. *Am J Public Health.* 1992;82:1658–1662.
3. Pitts DG, Cullen AP, Hacker PD. Ocular effects of ultraviolet radiation from 295 to 365 nm. *Invest Ophthalmol Vis Sci.* 1977;16:932–939.
4. Jose JG, Pitts DG. Wavelength dependency of cataracts in albino mice following chronic exposure. *Exp Eye Res.* 1985;41:545–563.
5. Söderberg PG. Acute cataract in the rat after exposure to radiation in the 300 nm wavelength region: a study of the macro-, micro- and ultrastructure. *Acta Ophthalmol (Copenh).* 1988;66:141–152.

6. Söderberg PG. Development of light dissemination in the rat lens after exposure to radiation in the 300 nm wavelength region. *Ophthalmic Res.* 1990;22:271-279.
7. Zigman S, Paxhia T, McDaniel T, Lou MF, Yu NT. Effect of chronic near-ultraviolet radiation on the gray squirrel lens in vivo. *Invest Ophthalmol Vis Sci.* 1991;32:1723-1732.
8. Hightower K, McCready J. Comparative effect of UVA and UVB on cultured rabbit lens. *Photochem Photobiol.* 1993;58:827-830.
9. Breadsell RO, Wegener A, Breipohl W. UV-B radiation-induced cataract in the royal collage of surgeons rat. *Ophthalmic Res.* 1994;26:84-89.
10. Wegener AR. In vivo studies on the effect of UV-radiation on the eye lens in animals. *Doc Ophthalmol.* 1994,88:221-232.
11. Michael R, Söderberg PG, Chen E. Long-term development of lens opacities after exposure to ultraviolet radiation at 300 nm. *Ophthalmic Res.* 1996;28:209-218.
12. Söderberg PG, Rol P, Denham DB, Parel J-M. Transmittance of the lens capsule. *Proc SPIE Ophthalmic Technologies VI.* 1996;2673: 21-24.
13. Hightower KR, Reddan JR, McCready JP, Dziedzic DC. Lens epithelium: a primary target of UVB irradiation. *Exp Eye Res.* 1994;59:557-564.
14. Wester U. Solar ultraviolet radiation on the Canary Islands and in Sweden: a comparison of irradiance levels. In: Paschier W, ed. *Human Exposure to UVR.* Amsterdam: Elsevier Science Publishers; 1987:275-279.
15. Michael R. Threshold dose estimation for ultraviolet radiation induced cataract. Stockholm: Karolinska Institutet; 1997. Thesis.
16. Wyllie AH. Apoptosis: an overview. *Br Med Bull.* 1997;53:451-465.
17. Kerr JF, Wyllie AH, Currie AR. Apoptosis: a basic biological phenomenon with wide-ranging implications in tissue kinetics. *Br J Cancer.* 1972;26:239-257.
18. Arends MJ, Wyllie AH. Apoptosis: mechanisms and roles in pathology. *Int Rev Exp Pathol.* 1991;32:223-254.
19. Alli R, Kleiman NJ. Detection of H_2O_2 and UV-B induced DNA single strand breaks by in-situ terminal deoxynucleotidyl (TdT) transferase analysis [ARVO Abstract]. *Invest Ophthalmol Vis Sci.* 1998;39(4):S319. Abstract nr 1473.
20. Grasl-Kraupp B, Ruttkay-Nedecky B, Koudelka H, Bukowska K, Bursch W, Schulte-Hermann R. In situ detection of fragmented DNA (TUNEL assay) fails to discriminate among apoptosis, necrosis, and autolytic cell death: a cautionary note. *Hepatology.* 1995; 21:1465-468.
21. Li WC, Spector A. Lens epithelial cell apoptosis is an early event in the development of UVB-induced cataract. *Free Radic Biol Med.* 1996;20:301-311.
22. Harocopos GJ, Kolker AE, Beebe DC. Is apoptosis associated with cataract formation in humans? [ARVO Abstract]. *Invest Ophthalmol Vis Sci.* 1996;37(3):S651. Abstract nr 3009.
23. Li WC, Kuszak JR, Dunn K, et al. Lens epithelial cell apoptosis appears to be a common cellular basis for non-congenital cataract development in humans and animals. *J Cell Biol.* 1995;130:169-181.
24. Söderberg PG. Experimental cataract induced by ultraviolet radiation. *Acta Ophthalmol Suppl.* 1990;68:23-28.
25. Negoescu A, Lorimier P, Labat-Moleur F, et al. In situ apoptotic cell labeling by the TUNEL method: improvement and evaluation on cell preparations. *J Histochem Cytochem.* 1996;44:959-968.
26. Cook B, Lewis GP, Fisher SK, Adler R. Apoptotic photoreceptor degeneration in experimental retinal detachment. *Invest Ophthalmol Vis Sci.* 1995;36:990-996.
27. Vrensen GFJM, Sanderson J, Willekens B, Duncan G. Calcium localization and ultrastructure of clear and pCMPS-treated rat lenses. *Invest Ophthalmol Vis Sci.* 1995;36:2287-2295.
28. Iwasaki K, Izawa M, Mihara M. UV-induced apoptosis in rat skin. *J Dermatol Sci.* 1996;12:31-35.
29. Baba T, Hanada K, Hashimoto I. The study of ultraviolet B-induced apoptosis in cultured mouse keratinocytes and in mouse skin. *J Dermatol Sci.* 1996;12:18-23.
30. Godar DE, Lucas AD. Spectral dependence of UV-induced immediate and delayed apoptosis: the role of membrane and DNA damage. *Photochem Photobiol.* 1995;62:108-113.
31. Söderberg PG, Philipson BT, Lindström B. Unscheduled DNA synthesis in lens epithelium after in vivo exposure to UV radiation in the 300 nm wavelength region. *Acta Ophthalmol (Copenh).* 1986; 64:162-168.
32. Spector A, Wang G, Wang R, Li W, Kleiman N. A brief photochemical induced oxidative insult causes irreversible lens damage and cataract, II: mechanism and action. *Exp Eye Res.* 1995;60:483-493.
33. Spector A, Kleiman NJ, Huang RR, Wang RR. Repair of H2O2-induced DNA damage in bovine lens epithelial cell cultures. *Exp Eye Res.* 1989;49:685-698.
34. Jose JG. The role of DNA damage, its repair and misrepair in the etiology of cataract: a review. *Ophthalmic Res.* 1978;10:52-62.
35. Godar DE. Preprogrammed and programmed cell death mechanisms of apoptosis: UV-induced immediate and delayed apoptosis. *Photochem Photobiol.* 1996;63:825-830.
36. Andley UP, Song Z, Wawrousek E, Bassnet S. Effect of expression of alpha-A crystallin on lens epithelial cell dynamics [ARVO Abstract]. *Invest Ophthalmol Vis Sci.* 1998;39(4):S8. Abstract nr 34.
37. Garcia-Porrero JA, Colvee E, Ojeda JL. The mechanisms of cell death and phagocytosis in the early chick lens morphogenesis: a scanning electron microscopy and cytochemical approach. *Anat Rec.* 1984;208:123-136.
38. Mikuni IKK. Phagocytosis of cultured human cataractous lens epithelial cells. *Nippon Ganka Gakkai Zasshi.* 1988;92:514-517.
39. Ishizaki Y, Voyvodic JT, Burne JF, Raff MC. Control of lens epithelial cell survival. *J Cell Biol.* 1993;121:899-908.
40. Kato K, Kurosaka D, Nagamoto T. Apoptotic cell death in rabbit lens after lens extraction. *Invest Ophthalmol Vis Sci.* 1997;38: 2322-2330.
41. Nickells RW, Zack DJ. Apoptosis in ocular disease: a molecular overview. *Ophthalmic Genet.* 1996;17:145-165.
42. Bär PR. Apoptosis-the cell's silent exit. *Life Sci.* 1996;59:369-378.
43. Zakeri ZF, Ahuja HS. Apoptotic cell death in the limb and its relationship to pattern formation. *Biochem Cell Biol.* 1994;72: 603-613.
44. Löfgren S, Michael R, Ayala M, Söderberg PG. Influence of pupil size and eye pigmentation on ultraviolet radiation-induced cataract [ICER Abstract]. *Exp Eye Res.* 1998;67(suppl 1):S140.
45. Boettner EA, Wolter JR. Transmission of ocular media. *Invest Ophthalmol.* 1962;1:776-783.
46. Söderberg PG, Löfgren S, Michael R, Gonzales-Cirre X. New method for measurement of in vivo penetration of UVR into the crystalline lens. *Proc SPIE Ophthalmic Technologies VIII.* 1998; 3246:43-47.
47. Bassnett S, Mataic D. Chromatin degradation in differentiating fiber cells of the eye lens. *J Cell Biol.* 1997;137:37-49.
48. Wyllie AH, Kerr JF, Currie AR. Cell death: the significance of apoptosis. *Int Rev Cytol.* 1980;68:251-306.
49. Kim J, Cha JH, Tisher CC, Madsen KM. Role of apoptotic and nonapoptotic cell death in removal of intercalated cells from developing rat kidney. *Am J Physiol.* 1996;270:F575-F592.
50. Iwanaga T, Hoshi O, Han H, Takahashi-Iwanaga H, Uchiyama Y, Fujita T. Lamina propria macrophages involved in cell death (apoptosis) of enterocytes in the small intestine of rats. *Arch Histol Cytol.* 1994;57:267-276.